NATIONAL ADVISORY COMMITTEE FOR AERONAUTICS

TECHNICAL MEMORANDUM 1414

AERODYNAMIC RESEARCH ON FUSELAGES WITH

RECTANGULAR CROSS SECTION

By K. Maruhn

Translation of "Aerodynamische Untersuchungen an Rümpfen mit
rechteckähnlichem Querschnitt." Jahrbuch 1942 der
deutschen Luftfahrtforschung

NACA

Washington
July 1958

AERODYNAMIC RESEARCH ON FUSELAGES WITH

RECTANGULAR CROSS SECTION[*]

By K. Maruhn

The influence of the deflected flow caused by the fuselage (especially by unsymmetrical attitudes) on the lift and the rolling moment due to sideslip has previously been discussed for infinitely long fuselages with circular and elliptical cross section. The aim of this work is to add rectangular cross sections and, primarily, to give a principle by which one can get practically usable contours through simple conformal mapping. In a few examples, the velocity field in the wing region and the induced flow produced are calculated and are compared with corresponding results from elliptical and strictly rectangular cross sections.

I. SYMBOLS (SEE FIGURE 1)

$t = y + iz$ points in the plane of the fuselage cross section

$\tau = \eta + i\zeta = \rho e^{i\vartheta}$ points in the plane of the mapped circle

b_R width of the rectangular contour (always taken as 2 in the examples)

h_R height of the rectangular contour, $\kappa = \dfrac{h_R}{b_R}$

s circular length on the contour measured from $t = 1$ in a positive sense (direction)

$v_\infty^{(t)}$ amount of flow velocity in the infinite t-plane

$v_\infty^{(\tau)}$ amount of flow velocity in the infinite τ-plane

$\alpha_\infty^{(t)}$ angle of flow in the infinite t-plane

$\alpha_\infty^{(\tau)}$ angle of flow in the infinite τ-plane

$w(t)$ velocity potential in the t-plane

$W(\tau)$ velocity potential in the τ-plane

v_y, v_z velocity components in the t-plane

p regional pressure

$p_\infty^{(t)}$ pressure in the infinite t-plane

$q^{(t)}$ dynamic pressure, formed with $V_\infty^{(t)}$

z_0 constant distance from the y-axis, or height of the
                        wing

b span of the elliptical wing

λ ratio of the span to the maximum chord of the
                        elliptical wing

Λ aspect ratio of the elliptical wing, $\dfrac{4\lambda}{\pi}$

β sideslip angle

c_L value of the rolling moment

II. INTRODUCTION

In order to find the influence of the fuselage on the wing in a first rough approximation, one determines the up-wash or down-wash field that is created by the fuselage boundary flow in the region of the wing (the wing momentarily assumed as being absent), hence the additional lift distribution, for example, and the additional moment of the wing. Of especial importance in respect to the lateral stability, is the rolling moment due to sideslip caused by sideslip of the fuselage. Research on this rolling moment due to sideslip has been done by a number of authors.[1] To simplify the research, an infinitely long fuselage with circular or elliptical cross section is generally treated. Inasmuch as some practical fuselages exhibit rectangular cross section, it might be of interest to do research on these contours, for which the fuselage is also taken as being infinitely long. The method of conformal mapping permits one, as will be shown in the following discussion, to obtain practically usable cross sections, without - as compared with the elliptical contour - having to do much more work to

[1] See Multhopp, H.: Zur Aerodynamik des Flugzeugrumpfes. Luftfahrtforschung, Bd. 18, Lfg. 2/3, Mar. 29, 1941, pp. 52-66. (Available as NACA TM 1036, 1942.) Jacobs, W.: Berechnung des Schiebe-Rollmomentes für Flügel-Rumpfanordnungen. Jahrbuch 1941 der dtsch. Luftfahrtforschung, vol. I, pp. 165-171.

determine all desired data. Comparisons with the results for the ellip-
tical cross section show that the influence of the corners, especially at
great height, is noticeable and is clearly seen during the rolling moment
due to sideslip. Calculations that were made for some cases on the exact
rectangle present a general idea of what effect a further sharpening of
the corners would have on the velocity field.

III. EQUATIONS FOR THE PRODUCTION OF CYLINDERS WITH RECTANGULAR

CROSS SECTION THROUGH CONFORMAL MAPPING

1. General

The next task is to determine rectangular figures in the t-plane
$(t = y + iz)$ (see fig. 1) that lie symmetrically to the y- and z-axes,
whose boundaries, through the use of the equation

$$t = a \left(\tau + c_0 + \frac{c_1}{\tau} + \frac{c_2}{\tau^2} - \ldots \right) \tag{1}$$

are shown as derived from the boundaries of the unit circle in the τ-plane
$(\tau = \eta + i\zeta = \rho e^{i\vartheta})$. If one now assumes - because of the symmetrical
qualities of the needed figures - that points in the t-plane lying
symmetrical to the axes are the same as symmetrical points in the τ-plane,
then, as one can easily see,

$$c_0 = c_2 = c_4 = \ldots = 0 \tag{2}$$

$$a, \; c_1, \; c_3, \; c_5, \; \ldots \; \text{real} \tag{3}$$

Equation (1) then reads

$$t = a \left(\tau + \frac{c_1}{\tau} + \frac{c_3}{\tau^3} + \ldots \right) \tag{4}$$

and gives the following parameter for the rectangle[2] in question

---

[2]In the following we use the term rectangle for the rectangular
figure with rounded corners to differentiate from the exact rectangle.

$$y = a\left[(1 + c_1)\cos \vartheta + c_3 \cos 3\vartheta + ...\right] \equiv g(\vartheta) \Bigg\}$$
$$z = a\left[(1 - c_1)\sin \vartheta - c_3 \sin 3\vartheta - . . . .\right] \equiv h(\vartheta) \Bigg\} \quad (5)$$

It is sufficient to regard these functions in the interval $0 \leqq \vartheta \leqq \pi/2$ because of the symmetry.

To reduce the mathematics involved, we now only use the case $c_7 = c_9 = . . . = 0$. Thus, we consider the mapping function

$$t = a\left(\tau + \frac{c_1}{\tau} + \frac{c_3}{\tau^3} + \frac{c_5}{\tau^5}\right) \quad (6)$$

and especially the parameter

$$y = a\left[(1 + c_1) \cos \vartheta + c_3 \cos 3\vartheta + c_5 \cos 5\vartheta\right] \Bigg\}$$
$$z = a\left[(1 - c_1) \sin \vartheta - c_3 \sin 3\vartheta - c_5 \sin 5\vartheta\right] \Bigg\} \quad (7)$$

As is shown in this equation, one can get very usable results even in the case $c_5 = 0$ (rectangle R_1); this means that only one more factor has to be used than for the ellipse. Expressions with $c_5 \neq 0$ were examined (rectangle R_2) to see what effects further factors would have.

The present constants c_1, c_3, and c_5 were then chosen so that the relationship κ = height: width = h_R: b_R of a basic exact rectangle is kept throughout, and so that in this rectangle (defined by eqs. (7)) the relationship fits as is best possible. The number $a > 0$ is only a scale factor and determines the size of the figure in the t-plane; if the definite body width b_R is used in equations (7), because $b_R/2 = g(0)$, the result is

$$a = \frac{\dfrac{b_R}{2}}{1 + c_1 + c_3 + c_5} \quad (8)$$

In the examples a is determined so that $\dfrac{b_R}{2} = 1$.

2. Equations Used to Determine c_1, c_3, and c_5

Without discussing in detail the derivation, which is found in part V, the equations used to find the constants of the desired shapes are put together by using a given κ-value

1. Rectangle R_1: $\left(t = a\left(\tau + \dfrac{c_1}{\tau} + \dfrac{c_3}{\tau^3} \right) \right)$

   (a) $0 < \kappa \leqq 1$:

$$c_3 = -\frac{\kappa}{4 + 5\kappa}, \quad c_1 = 1 + 9c_3$$

   (b) $1 \leqq \kappa < \infty$ (practical common value):

$$c_3 = -\frac{1}{5 + 4\kappa}, \quad c_1 = -1 - 9c_3$$

2. Rectangle R_2: $\left(t = a\left(\tau + \dfrac{c_1}{\tau} + \dfrac{c_3}{\tau^3} + \dfrac{c_5}{\tau^5} \right) \right)$

   (a) $0 < \kappa \leqq \dfrac{8}{17}$:

$$c_5 = -\frac{3\kappa}{64 + 89\kappa}, \quad c_1 = 50c_5 + 1, \quad c_3 = \frac{25c_5}{3}$$

   (b) $\dfrac{8}{17} \leqq \kappa \leqq \dfrac{17}{8}$ (practical common value):

$$c_5 = \frac{1}{27}\frac{\kappa - 1}{\kappa + 1}, \quad c_1 = -25c_5, \quad c_3 = -\frac{1}{9}$$

   (c) $\dfrac{17}{8} \leqq \kappa < \infty$:

$$c_5 = \frac{3}{89 + 64\kappa}, \quad c_1 = 50c_5 - 1, \quad c_3 = -\frac{25c_5}{3}$$

Worked examples:

1. $\kappa = 1$: $c_3 = -\frac{1}{9}$, $c_1 = 0$, $a = \frac{9}{8}$ (square Q)

$\kappa = 1.5$: $c_3 = -\frac{1}{11}$, $c_1 = -\frac{2}{11}$, $a = \frac{11}{8}$

2. $\kappa = 1$: $c_5 = 0$, $c_1 = 0$, $c_3 = -\frac{1}{9}$, $a = \frac{9}{8}$

$\kappa = 1.5$: $c_5 = \frac{1}{135}$, $c_1 = -\frac{5}{27}$, $c_3 = -\frac{1}{9}$, $a = \frac{45}{32}$

In the case $\kappa = 1$, R_1 and R_2 automatically coincide with the square Q. (See fig. 2 where the corresponding circle and the exact square Q_{ex} are shown for comparison.) The cases $\kappa = 1.5$ are shown in figure 3 together with the corresponding ellipse and the exact rectangle R_{ex}. It can be shown that R_1 and R_2 will be an increasing distance apart as κ exceeds 1.

IV. USE OF FLOW FREE OF CIRCULATION

1. General Equations for v_y and v_z in Case of an
Expression of the Form $t = a\left(\tau + \frac{c_1}{\tau} + \frac{c_3}{\tau^3} + \frac{c_5}{\tau^5}\right)$

If $W(\tau)$ describes the velocity potential of the circular flow in the τ-plane, ($\tau = \rho e^{i\vartheta}$), one arrives at the velocity field in the t-plane, since $w(t)$ is the velocity potential existing there, from the equation

$$\frac{dw}{dt} = \frac{dW}{d\tau}\frac{1}{\frac{dt}{d\tau}} \tag{9}$$

Furthermore, if $V_\infty^{(t)}$ and $\alpha_\infty^{(t)}$, (or $V_\infty^{(\tau)}$ and $\alpha_\infty^{(\tau)}$) (see fig. 1) stand for the velocity and direction of the flow (relative to the negative real axis) at infinity of the t- (or τ-) plane, then

$$V_\infty^{(\tau)} = \left|t'(\infty)\right| V_\infty^{(t)} \tag{10}$$

is generally true if these points correspond to each other.

In the special case

$$t = a\left(\tau + \frac{c_1}{\tau} + \frac{c_3}{\tau^3} + \frac{c_5}{\tau^5}\right) \tag{11}$$

the velocity components v_y and v_z of the flow in the t-plane for $\alpha_\infty^{(t)} = 0$ (flow parallel to the negative y-axis) are derived from

$$\frac{v_y}{V_\infty^{(t)}} = -\frac{1}{N}\left\{1 + \frac{c_1}{\rho^4} + \left(\frac{3c_3}{\rho^6} - \frac{1 + c_1}{\rho^2}\right)\cos 2\vartheta + \left(\frac{5c_5}{\rho^8} - \frac{3c_3}{\rho^4}\right)\cos 4\vartheta - \right.$$

$$\left. \frac{5c_5}{\rho^6}\cos 6\vartheta\right\} \tag{12}$$

$$\frac{v_z}{V_\infty^{(t)}} = \frac{1}{N}\left\{\left(\frac{1 - c_1}{\rho^2} + \frac{3c_3}{\rho^6}\right)\sin 2\vartheta + \left(\frac{5c_5}{\rho^8} - \frac{3c_3}{\rho^4}\right)\sin 4\vartheta - \frac{5c_5}{\rho^6}\sin 6\vartheta\right\} \tag{13}$$

with

$$N = 1 + \frac{c_1^2}{\rho^4} + \frac{9c_3^2}{\rho^8} + \frac{25c_5^2}{\rho^{12}} + 2\left(\frac{3c_1c_3}{\rho^6} + \frac{15c_3c_5}{\rho^{10}} - \frac{c_1}{\rho^2}\right)\cos 2\vartheta + $$

$$2\left(\frac{5c_1c_5}{\rho^8} - \frac{3c_3}{\rho^4}\right)\cos 4\vartheta - \frac{10c_5}{\rho^6}\cos 6\vartheta$$

while in the case $\alpha_\infty^{(t)} = \pi/2$ (flow parallel to the positive z-axis)

$$\frac{v_y}{V_\infty^{(t)}} = -\frac{1}{N}\left\{\left(\frac{1 + c_1}{\rho^2} + \frac{3c_3}{\rho^6}\right)\sin 2\vartheta + \left(\frac{3c_3}{\rho^4} + \frac{5c_5}{\rho^8}\right)\sin 4\vartheta + \frac{5c_5}{\rho^6}\sin 6\vartheta\right\} \tag{14}$$

$$\frac{v_z}{V_\infty^{(t)}} = \frac{1}{N}\left\{1 - \frac{c_1}{\rho^4} + \left(\frac{1 - c_1}{\rho^2} - \frac{3c_3}{\rho^6}\right)\cos 2\vartheta - \left(\frac{3c_3}{\rho^4} + \frac{5c_5}{\rho^8}\right)\cos 4\vartheta - \frac{5c_5}{\rho^6}\cos 6\vartheta\right\} \tag{15}$$

are obtained. If one wants to find v_y and v_z in particular points of the t-plane, one must, of course, first find the corresponding values $\tau = \rho e^{i\vartheta}$ by using the reverse of equation (11).

2. Results of Calculations

(a) <u>Velocity fields</u>.- As proved by equations (12) to (15), (for $\kappa = 1$ and $\kappa = 1.5$) v_y and v_z on the parallels drawn[3] at an interval of $z_0 = 0$, $\frac{h_R}{8}$, $\frac{h_R}{4}$, $\frac{3h_R}{8}$, $\frac{h_R}{2}$ on the y-axis were calculated for the examples listed in part III; the results are shown in figures 4, 5, and 11 to 14. In figures 6 to 10 and 15 to 23, the results are compared with the corresponding flow around an ellipse and (in some cases) around an exact rectangle[4]. One can then readily see that, excepting the vicinity of the corner, the velocity fields of the rectangle and the R_{ex} (in this case Q and Q_{ex}) differ comparatively little. The difference in the field around an ellipse (or a circle) is greater. Figures 24 to 26 show the pressure distribution on the contours plotted against the body length; in these plots, the effect of the corners is especially noticeable.

(b) <u>Induced rolling moment</u>.- The results from (a) were finally used to determine the rolling moment due to sideslip caused by the boundary-layer flow, exerted by inclined flow on an elliptical wing. This was to be done by using the method mentioned in the introduction, in which the influence of the induced moment on the wing is not considered. The calculation was carried out for the following examples ($c'_{a\infty} = 5.5$)[*]:

1. $\Lambda = 12.7$ $\lambda = 10$ $b_R/b = 1/15$ (High aspect ratio)

2. $\Lambda = 7.6$ $\lambda = 6$ $b_R/b = 1/12$ (Medium aspect ratio)

3. $\Lambda = 3.8$ $\lambda = 3$ $b_R/b = 1/6$ (Low aspect ratio)

and was based on the equation

---

[3]In the determination of τ from equation (11), it proved practical to assume ρ and to calculate ϑ through successive approximations from $\tau_1 = \frac{t}{a}$, $\tau_2 = \frac{t}{a} - \frac{c_1}{\tau_1} - \frac{c_3}{\tau_1^3} - \frac{c_5}{\tau_1^5}$, . . . since this did not depend on finding v_y and v_z at determined points of these parallels.

[4]See Birkley, G.: Two-Dimensional Potential Problems for the Space Outside a Rectangle. Proc. London Math. Soc., (2), 37, 1934, pp. 82-105. Here the conformal mapping of the boundary field of an exact rectangle on the outside of a unit circle is made calculable. The necessary calculations are of course considerably more extensive than on our figures R_1 and R_2.

[*]NACA reviewer's note: $c'_{a\infty}$ may be defined as section lift curve slope.

$$\frac{dc_L}{d\beta} = - \frac{32\lambda}{\pi\left(\frac{4\lambda}{c'_{a\infty}} + 2\right)b^2} \int_{-b/2}^{b/2} \frac{v_z}{v_\infty^{(t)}} \sqrt{1 - \left(\frac{2y}{b}\right)^2} \, y \, dy \qquad [5] \qquad (16)$$

The results, shown in figures 27 to 29, were calculated for different fuselage shapes for which the widths were assumed to be equal ($b_R = 2$). The results, excepting those concerning the circle, were found through graphical integration, where in the interval -1 to 1 (fuselage width) $v_z/v_\infty^{(t)} = 0$ was assumed for all high positions. The results show a strong influence on the corners, besides the great influence of the high position. The differences from the ellipse (or the circle) are noticeable; the rectangles R_1 and R_2, however, show only small differences so that, in general, the simpler shape R_1 should be sufficient.

V. DERIVATIONS OF EQUATIONS IN PART III

1. General

To achieve a reasonably rectangular figure, one must assume (see eqs. (5)) that, for $0 < \vartheta < \pi/2$,

$$g(\vartheta), \ h(\vartheta) > 0, \quad g'(\vartheta) < 0, \quad h'(\vartheta) > 0 \ldots \qquad (17)$$

is true. In the end points of the interval, equal marks can be used. We further want to avoid points of inflection on the needed contour; then, because of

$$\frac{dz}{dy} = \frac{h'(\vartheta)}{g'(\vartheta)}$$

$$\frac{d^2z}{dy^2} = \frac{g'h'' - h'g''}{(g')^3}$$

$$\text{or} \quad \frac{dy}{dz} = \frac{g'}{h'}$$

$$\frac{d^2y}{dz^2} = \frac{h'g'' - g'h''}{(h')^3} \ldots \qquad (18)$$

---

[5]Equation (16) is derived from the known equation for the rolling moment of an elliptical wing, if one replaces the geometrical angle (of attack) by $\frac{v_z}{v_\infty^{(t)}}$.

of course

$$g'(\vartheta)h''(\vartheta) - h'(\vartheta)g''(\vartheta) > 0 \quad \left(0 < \vartheta < \frac{\pi}{2}\right) \tag{19}$$

is proved.

The range of values of the numbers c_1, c_3, ... is subject then to certain restrictions that result from conditions (17) and (19); they are defined by the fixed side ratio of the rectangle and through the hypothesis that, for $\vartheta = 0$ and $\vartheta = \pi/2$, the contour will have flat points.[6]

---

[6]A curve $y(x)$ (or $x(y)$) has a flat point of the nth order (n odd) in x_0 (or y_0) if y (or x) is differentiable $(n + 2)$ times and $y''(x_0) = y'''(x_0) = \ldots = y^{(n+2)}(x_0) = 0$ (or $x''(y_0) = x'''(y_0) = \ldots = x^{(n+2)}(y_0 = 0)$) is valid. If in this case the flat points for $\vartheta = 0$ (or $\vartheta = \pi/2$) should enter, then through continuation of the differentiation started in equation (18), it is shown that because of

$$g'(0) = g'''(0) = \ldots = 0 \quad \left(\text{or } h'\left(\frac{\pi}{2}\right) = h'''\left(\frac{\pi}{2}\right) = \ldots = 0\right)$$

$$\left.\frac{dy}{dz}\right|_{\vartheta=0} = \left.\frac{d^3y}{dz^3}\right|_{\vartheta=0} = \ldots = 0$$

$$\text{or} \quad \left.\frac{dz}{dy}\right|_{\vartheta=\frac{\pi}{2}} = \left.\frac{d^3z}{dy^3}\right|_{\vartheta=\frac{\pi}{2}} = \ldots = 0$$

is always automatically satisfied if $h'0 \neq 0$ (or $g'\left(\frac{\pi}{2}\right) \neq 0$) and that with respect to equation (17), $h'(0) > 0$ (or $g'\left(\frac{\pi}{2}\right) < 0$) is true. In order that

$$\left.\frac{d^2y}{dz^2}\right|_{\vartheta=0} = \left.\frac{d^4y}{dz^4}\right|_{\vartheta=0} = \ldots = \left.\frac{d^{n+1}y}{dz^{n+1}}\right|_{\vartheta=0} = 0$$

$$\text{or} \quad \left.\frac{d^2z}{dy^2}\right|_{\vartheta=\frac{\pi}{2}} = \left.\frac{d^4z}{dy^4}\right|_{\vartheta=\frac{\pi}{2}} = \ldots = \left.\frac{d^{n+1}z}{dz^{n+1}}\right|_{\vartheta=\frac{\pi}{2}} = 0$$

be valid, the relationships $g''(0) = g''''(0) = \ldots = g^{(n+1)}(0) = 0$ (or $h''\left(\frac{\pi}{2}\right) = h''''\left(\frac{\pi}{2}\right) = \ldots = h^{(n+1)}\left(\frac{\pi}{2}\right) = 0$) must exist.

As already stated in part III, our representative equation (4) should show the boundary field of the desired shape clearly conforming to the circumference of the unit circle of the τ-plane; this condition is fulfilled when the constants c_1, c_3, . . . are so taken that $t'(\tau)$ is different from zero in the entire boundary field.[7] Now one has only to prove that the derived representative function will be sufficient to accomodate this restriction.

One will naturally attempt to use as few factors as possible in equation (1) - that is, with flat points of a low order for $\vartheta = 0$ and $\vartheta = \pi/2$. As was shown in part III, the expressions up to and including c_3/τ^3 and c_5/z^{5*} give useable values. To add further factors would probably not improve the quality of a rectangular fuselage cross section; certainly such an extension would not develop any difficulties and could be performed without complications in the following way.

$$2. \text{ The Rectangle } R_1 \left(t = a\left(\tau + \frac{c_1}{\tau} + \frac{c_3}{\tau^3}\right)\right)$$

The equations brought forward from equations (5) for $g(\vartheta)$ and $h(\vartheta)$ are:

$$\left.\begin{aligned}
g(\vartheta) &= a\left[(1 + c_1) \cos \vartheta + c_3 \cos 3\vartheta\right] \\
h(\vartheta) &= a\left[(1 - c_1) \sin \vartheta - c_3 \sin 3\vartheta\right]
\end{aligned}\right\} \tag{20}$$

We choose a flat point of the first order for $\vartheta = 0$; then, (see footnote 6) $h'(0) > 0$. Therefore

$$1 - c_1 - 3c_3 > 0 \tag{21}$$

and further $g''(0) = -a\left[(1 + c_1) + 9c_3\right] = 0$, that is,

$$c_1 = -1 - 9c_3 \tag{22}$$

---

[7]See Schmidt, B. Harry: Aerodynamik des Fluges. (Berlin and Leipzig), 1929, p. 98.

*NACA reviewer's note: The expression should read c_5/τ^5. (See eq. (6).)

must be true. Of course, $\left.\dfrac{dz}{dy}\right|_{\vartheta=\frac{\pi}{2}}$ is then equal to 0, which is the case when $g'\left(\dfrac{\pi}{2}\right) < 0$ or

$$1 + c_1 - 3c_3 > 0 \tag{23}$$

This and the deduction (21) is correct, with reference to equation (22) if

$$-\frac{1}{3} < c_3 < 0 \tag{24}$$

is true. The still available constant c_3 is needed to determine the necessary side ratio κ of the rectangle. From equations (20) one derives, taking equation (22) into account, at

$$\kappa = \frac{h_R}{b_R} - \frac{h\left(\dfrac{\pi}{2}\right)}{g(0)} = -\frac{1 + 5c_3}{4c_3} \tag{25}$$

or

$$c_3 = -\frac{1}{5 + 4\kappa} \tag{26}$$

Finally, the field of values for c_3 and, therefore, also for κ must be found, for which field the restrictions in equations (17) and (19) are taken care of. For this purpose we write g and h in the form

$$\left.\begin{aligned} g(\vartheta) &= a\left[\left(1 + c_1 - 3c_3\right)\cos\vartheta + 4c_3\cos^3\vartheta\right] \\ h(\vartheta) &= a\left[\left(1 - c_1 - 3c_3\right)\sin\vartheta + 4c_3\sin^3\vartheta\right] \end{aligned}\right\} \tag{27}$$

from which, with reference to equation (22), we get

$$\left.\begin{aligned} g(\vartheta) &= -4ac_3\left[3\cos\vartheta - \cos^3\vartheta\right] \\ h(\vartheta) &= 2a\left[\left(1 + 3c_3\right)\sin\vartheta + 2c_3\sin^3\vartheta\right] \end{aligned}\right\} \tag{28}$$

Further,

$$g'(\vartheta) = 12ac_3 \sin^3 \vartheta$$
$$h'(\vartheta) = 2a\left[(1 + 9c_3) \cos \vartheta - 6c_3 \cos^3 \vartheta\right] \tag{29}$$

and

$$g''(\vartheta) = 36ac_3 \sin^2 \vartheta \cos \vartheta$$
$$h''(\vartheta) = -2a \sin \vartheta\left[1 + 9c_3 - 18c_3 \cos^2 \vartheta\right] \tag{30}$$

are true. To make the functions $g(\vartheta)$, $h(\vartheta) > 0$ for $0 < \vartheta < \frac{\pi}{2}$

$$-\frac{1}{5} < c_3 < 0 \tag{31}$$

must be valid. (See eqs. (28).) Then $g' < 0$ is also correct (see eqs. (29)), while the expression $h' > 0$ requires that, for all values of ϑ when $0 < \vartheta < \frac{\pi}{2}$, the expression $1 + 3c_3(3 - 2 \cos^2 \vartheta) > 0$, that is,

$$c_3 \geqq -\frac{1}{9} \tag{32}$$

is true. As one can easily calculate, equations (29) and (30) give

$$g'h'' - h'g'' = -24a^2c_3 \sin^2 \vartheta\left(1 + 9c_3 + 2 \cos^2 \vartheta\right), \ldots \tag{33}$$

and one can see that condition (19) is satisfied if $c_3 < 0$ and $1 + 9c_3 + 2 \cos^2 \vartheta > 0$; therefore,

$$-\frac{1}{9} \leqq c_3 < 0 \tag{34}$$

is true. These equations also satisfy conditions (24), (31), and (32). Condition (34) stands for the field of values

$$1 \leqq \kappa < \infty \tag{35}$$

for κ because of equation (25). Taking equation (22) into account,

$$t'(\tau) = a\left(1 + \frac{1 + 9c_3}{\tau^2} - \frac{3c_3}{\tau^4}\right) \tag{36}$$

is true; therefore, in consideration of condition (34),

$$|t'(\tau)| \geqq a\left(1 - \left|\frac{1 + 9c_3}{\tau^2}\right| - \left|\frac{3c_3}{\tau^4}\right|\right) \geqq a\left[1 - (1 + 9c_3) + 3c_3\right] = -6ac_3 > 0 \tag{37}$$

is found for $|\tau| \geqq 1$; the zero points of $t'(\tau)$ lie inside the circle $|\tau| = 1$.

As one notices in further analysis, the assumption that the flat point of the first order lies at $\vartheta = \frac{\pi}{2}$, at $c_1 = 1 + 9c_3$, and $\kappa = -\frac{4c_3}{1 + 5c_3}$ (in this case $c_3 = -\frac{\kappa}{4 + 5\kappa}$). To satisfy conditions (17) and (19) $0 > c_3 \geqq -\frac{1}{9}$ must apply here, which for κ corresponds to the interval $0 < \kappa \leqq 1$.

From the preceding discussion it is seen that the unit circle can actually be changed into rectangular figures of any desirable side ratio through the use of the representative equation $t = a\left(\tau + \frac{c_1}{\tau} + \frac{c_3}{\tau^3}\right)$. Information about its practical use is given by the examples in part IV.

3. The Rectangle R_2 $\left(t = a\left(\tau + \frac{c_1}{\tau} + \frac{c_3}{\tau^3} + \frac{c_5}{\tau^5}\right)\right)$

(a) <u>Two flat points of first order.</u>- We now set:

$$\left.\begin{aligned} g(\vartheta) &= a\left[(1 + c_1)\cos\vartheta + c_3\cos 3\vartheta + c_5\cos 5\vartheta\right] \\ h(\vartheta) &= a\left[(1 - c_1)\sin\vartheta - c_3\sin 3\vartheta - c_5\sin 5\vartheta\right] \end{aligned}\right\} \tag{38}$$

and assume one flat point of the first order for each $\vartheta = 0$ and $\vartheta = \frac{\pi}{2}$; this means the functions $g''(0) = h''\left(\frac{\pi}{2}\right) = 0$ must apply (see footnote 6), or

$$1 + c_1 + 9c_3 + 25c_5 = 0 \qquad 1 - c_1 + 9c_3 - 25c_5 = 0 \tag{39}$$

under the restrictions $h'(0) > 0$, $g'\left(\frac{\pi}{2}\right) < 0$, that is

$$1 - c_1 - 3c_3 - 5c_5 > 0 \qquad 1 + c_1 - 3c_3 + 5c_5 > 0 \tag{40}$$

must be true. From equations (39)

$$c_3 = -\frac{1}{9} \qquad c_1 = -25c_5 \tag{41}$$

follows and with these values condition (40) is satisfied for

$$-\frac{1}{15} < c_5 < \frac{1}{15} \tag{42}$$

The still unused constant c_5 is again used for the side ratio. As one can see from equations (38) and equation (41),

$$\kappa = \frac{1 + 27c_5}{1 - 27c_5} \qquad c_5 = \frac{1}{27}\frac{\kappa - 1}{\kappa + 1} \tag{43}$$

We now determine the restrictions to which c_5 and therefore κ (because of equations (17) and (19)) are subject. A little calculation, in consideration of equation (41), results in

$$\left.\begin{aligned}
g(\vartheta) &= a\left[\left(\frac{4}{3} - 20c_5\right)\cos\vartheta - \left(\frac{4}{9} + 20c_5\right)\cos^3\vartheta + 16c_5\cos^5\vartheta\right] \\
h(\vartheta) &= a\left[\left(\frac{4}{3} + 20c_5\right)\sin\vartheta - \left(\frac{4}{9} - 20c_5\right)\sin^3\vartheta - 16c_5\sin^5\vartheta\right]
\end{aligned}\right\} \tag{44}$$

$$\left.\begin{aligned}
g'(\vartheta) &= -4a\sin^3\vartheta\left(\frac{1}{3} - 25c_5 + 20c_5\sin^2\vartheta\right) \\
h'(\vartheta) &= 4a\cos^3\vartheta\left(\frac{1}{3} + 25c_5 - 20c_5\cos^2\vartheta\right)
\end{aligned}\right\} \tag{45}$$

$$g''(\vartheta) = -4a \sin^2 \vartheta \cos \vartheta \left(1 - 75c_5 + 100c_5 \sin^2 \vartheta\right)$$
$$h''(\vartheta) = -4a \cos^2 \vartheta \sin \vartheta \left(1 + 75c_5 - 100c_5 \cos^2 \vartheta\right) \tag{46}$$

from which

$$g'h'' - h' g'' = 16a^2 \sin^2 \vartheta \cos^2 \vartheta \left[\frac{1}{3} + 20c_5 - 375c_5^2 - 40c_5 \cos^2 \vartheta\right] \tag{47}$$

is derived. One can easily see that for $0 < \vartheta < \frac{\pi}{2}$, $g' < 0$ and $h' > 0$ are definitely satisfied if

$$-\frac{1}{75} \leqq c_5 \leqq \frac{1}{75} \tag{48}$$

is true. For these values $g(\vartheta)$, $h(\vartheta) > 0$. The expression (47) is positive for $|c_5| = \frac{1}{75}$ in the interval $0 < \vartheta < \frac{\pi}{2}$; because of the construction of the quadratic equation in equation (47) on the right side in the square brackets, this equation applies to the entire interval (48). Restrictions (17) and (19) are hereby satisfied if c_5 is subject to restriction (48); therefore, the side ratio is within the interval

$$\frac{8}{17} \leqq \kappa \leqq \frac{17}{8} \tag{49}$$

which should take care of the field in question for practical fuselage cross sections.

To discuss the position of the zero places of $t'(\tau)$ before concluding, we write our representative equations with respect to equations (41) in the form

$$t(\tau) = a\left(\tau - \frac{25c_5}{\tau} - \frac{1}{9\tau^3} + \frac{c_5}{\tau^5}\right) \tag{50}$$

Because of expression (48) we derive for $|\tau| \geqq 1$

$$|t'(\tau)| = a\left|1 + \frac{25c_5}{\tau^2} + \frac{1}{3\tau^4} - \frac{5c_5}{\tau^6}\right| \geqq a\left(1 - \frac{1}{3} - \frac{1}{3} - \frac{1}{15}\right) > 0 \tag{51}$$

The zero places for $t'(\tau)$ lie inside the circle $|\tau| = 1$.

(b) <u>A flat point of the third order</u>.- Another method of determining the available constants consists of assuming one flat point of the third order instead of two flat points of the first order for $\vartheta = 0$ or $\vartheta = \frac{\pi}{2}$ It will be shown that the side ratios not included in expression (49) can hereby be derived; this case will be briefly discussed.

If the flat point for $\vartheta = 0$ is used, then

$$1 + c_1 + 9c_3 + 25c_5 = 0 \quad \text{and} \quad 1 + c_1 + 81c_3 + 625c_5 = 0 \tag{52}$$

or

$$c_3 = -\frac{25}{3} c_5 \qquad c_1 = 50c_5 - 1 \tag{53}$$

is correct. Since restriction (40) is satisfied because of $h'(0) > 0$, $g'\left(\frac{\pi}{2}\right) < 0$, the limits for c_5

$$0 < c_5 < \frac{1}{15} \tag{54}$$

are hereby found. Taking into consideration equations (53), we have

$$\left.\begin{array}{l} g(\vartheta) = 16ac_5\left(5 \cos \vartheta - \frac{10}{3} \cos^3 \vartheta + \cos^5 \vartheta\right) \\[2mm] h(\vartheta) = 2a\left[\left(1 - 15c_5\right) \sin \vartheta - \frac{20}{3} c_5 \sin^3 \vartheta + 8c_5 \sin^5 \vartheta\right] \end{array}\right\} \tag{55}$$

$$\left.\begin{array}{l} g'(\vartheta) = -80ac_5 \sin^5 \vartheta \\[2mm] h'(\vartheta) = 2a\left[\left(1 - 75c_5\right) \cos \vartheta + 100c_5 \cos^3 \vartheta - 40c_5 \cos^5 \vartheta\right] \end{array}\right\} \tag{56}$$

$$\left.\begin{array}{l} g''(\vartheta) = -400ac_5 \sin^4 \vartheta \cos \vartheta \\[2mm] h''(\vartheta) = -2a \sin \vartheta\left[1 - 75c_5 + 300c_5 \cos^2 \vartheta - 200c_5 \cos^4 \vartheta\right] \end{array}\right\} \tag{57}$$

and

$$g'h'' - h'g'' = 160a^2c_5 \sin^4 \vartheta \left(1 + 4 \cos^2 \vartheta - 75c_5\right) \tag{58}$$

and without much trouble one finds that for

$$0 < c_5 \lessgtr \frac{1}{75} \tag{59}$$

restrictions (17) and (19) are satisfied. In respect to

$$\kappa = \frac{3 - 89c_5}{64c_5} \quad \text{or} \quad c_5 = \frac{3}{64\kappa + 89} \tag{60}$$

this corresponds to the κ-interval

$$\frac{17}{8} \leqq \kappa < \infty \tag{61}$$

with which the connection to the right side of equation (49), is established.

The representative function then is

$$t(\tau) = a\left(\tau + \frac{50c_5 - 1}{\tau} - \frac{25c_5}{3\tau^3} + \frac{c_5}{\tau^5}\right) \tag{62}$$

Therefore, with $|\tau| \geqq 1$, keeping condition (59) in mind,

$$\left| t'(\tau) \right| = a\left| 1 + \frac{1 - 50c_5}{\tau^2} + \frac{25c_5}{\tau^4} - \frac{5c_5}{\tau^6} \right| \geqq a\left[1 - \left(1 - 50c_5\right) - 25c_5 - 5c_5 \right] > 0 \tag{63}$$

is correct. If the flat point of the third order lies on the point $\vartheta = \frac{\pi}{2}$

$$\left.\begin{array}{cc} c_1 = 1 + 50c_5 & c_3 = \frac{25}{3} c_5 \\[2ex] \kappa = -\dfrac{64c_5}{3 + 89c_5} \quad \text{or} \quad c_5 = -\dfrac{3\kappa}{64 + 89\kappa} \end{array}\right\} \tag{64}$$

is found with the restrictions

$$-\frac{1}{75} \leqq c_5 < 0 \quad \text{or} \quad 0 < \kappa \leqq \frac{8}{17} \tag{65}$$

Translated by Peter R. Kurzhals
National Advisory Committee
for Aeronautics
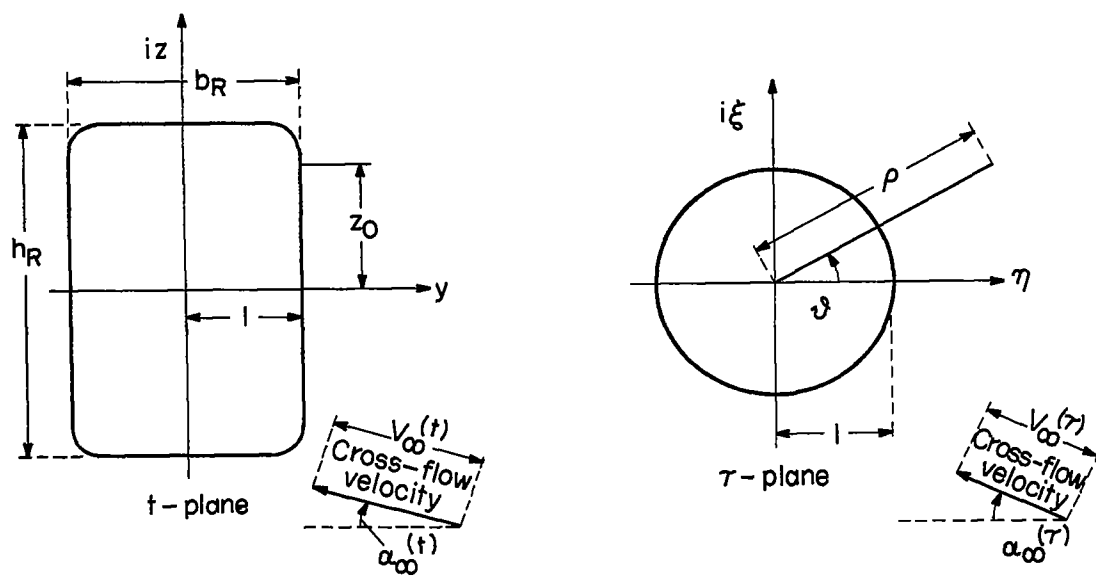
Figure 1.- Illustration of the symbols.
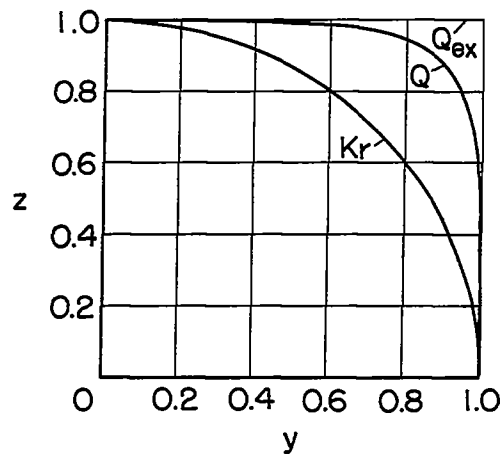
Figure 2. - First quadrant with circle (Kr), square Q, and the exact square Q_{ex} ($\kappa = 1$).
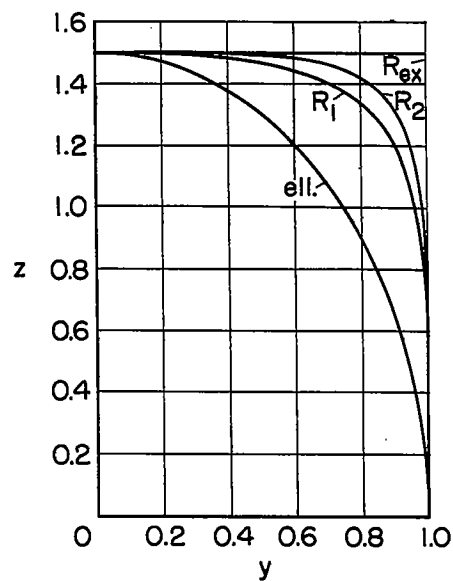
Figure 3.- First quadrant with ellipse (ell.), rectangle R_1, rectangle R_2, and exact rectangle R_{ex} ($\kappa = 1.5$).
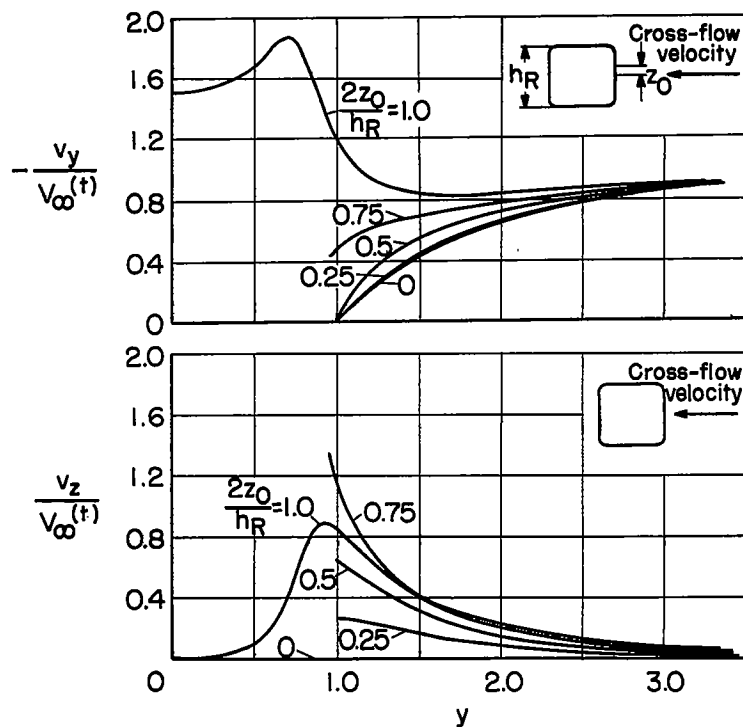
Figure 4.- Velocity field for the square Q in flow $\alpha_\infty^{(t)} = 0°$.
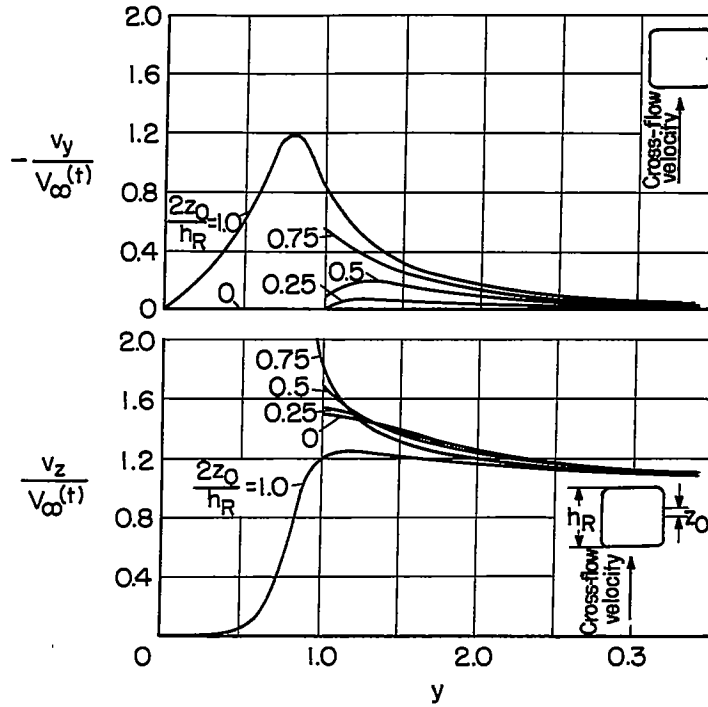
Figure 5.- Velocity field for the square Q in flow $\alpha_\infty^{(t)} = 90^\circ$.
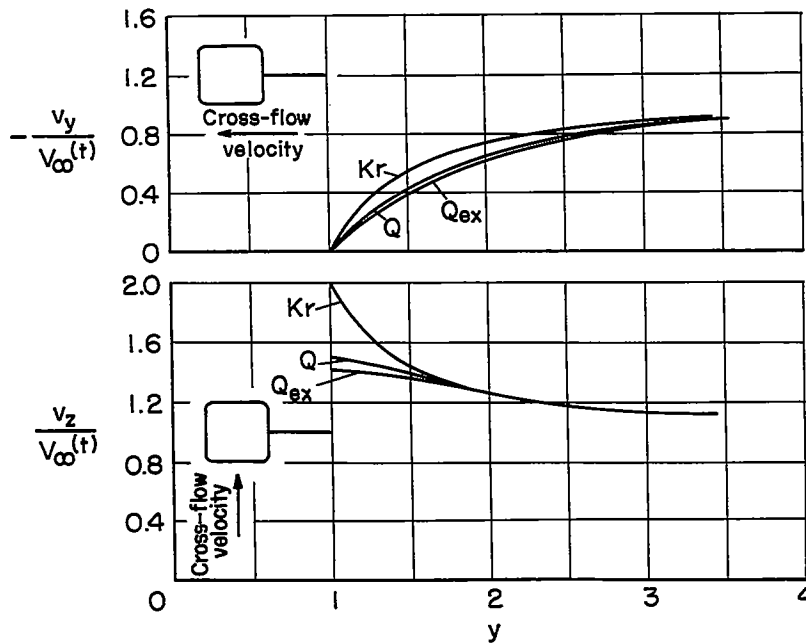
Figure 6.- Velocity field, comparison between circle, Q and Q_{ex}.
$2z_0/h_R = 0$ $\alpha_\infty^{(t)} = 0^\circ$, 90°.
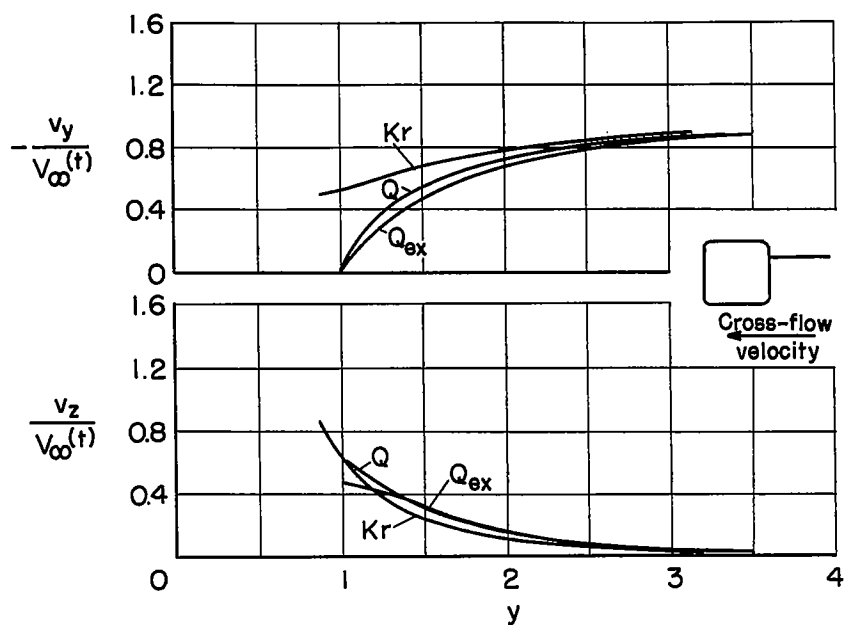
Figure 7.- Velocity field, comparison between circle, Q and Q_{ex}. $2z_0/h_R = 0.5$ $\alpha_\infty^{(t)} = 0^\circ$.
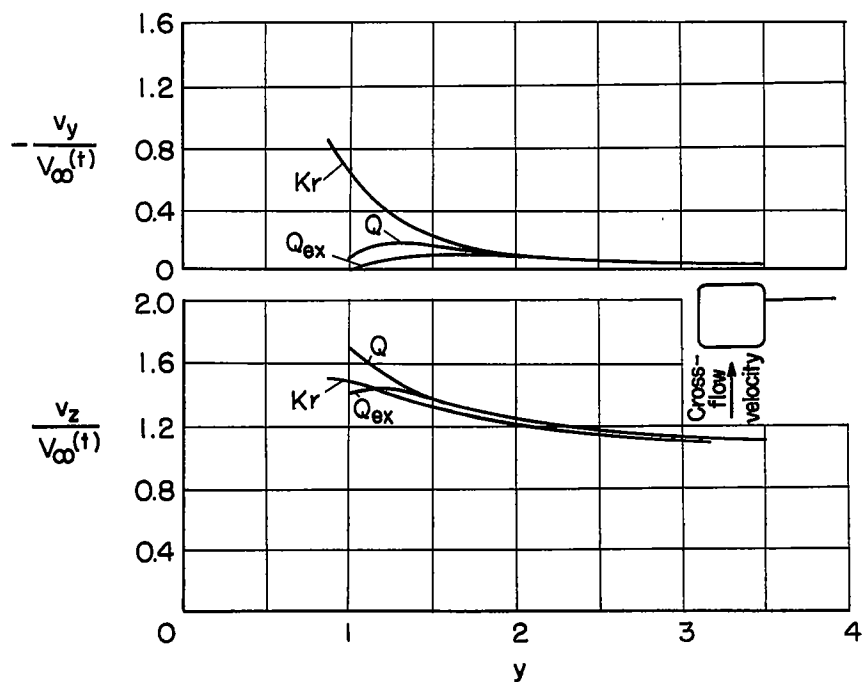
Figure 8.- Velocity field, comparison between circle, Q and Q_{ex}. $2z_0/h_R = 0.5$ $\alpha_\infty^{(t)} = 90^\circ$.
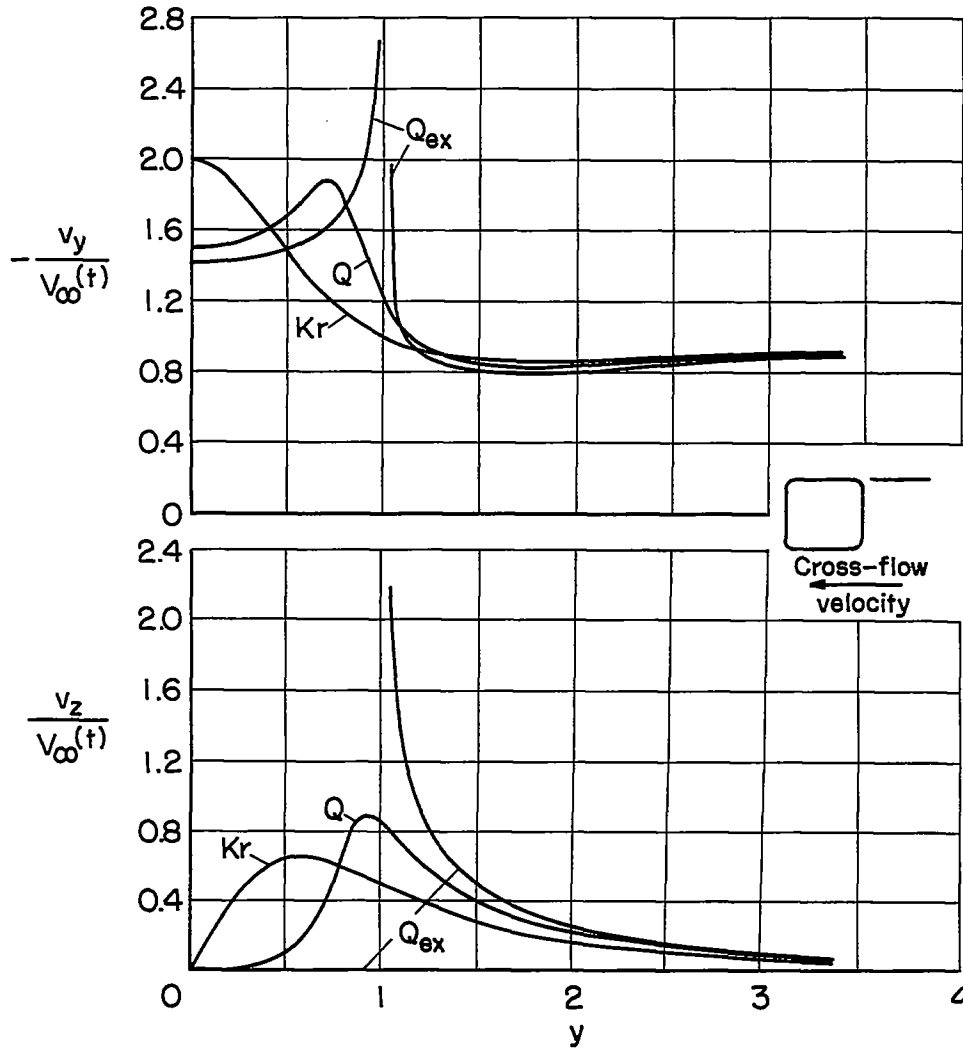
Figure 9.— Velocity field, comparison between circle, Q and Q_{ex}.
$2z_0/h_R = 1$ $\alpha_\infty^{(t)} = 0^0$.
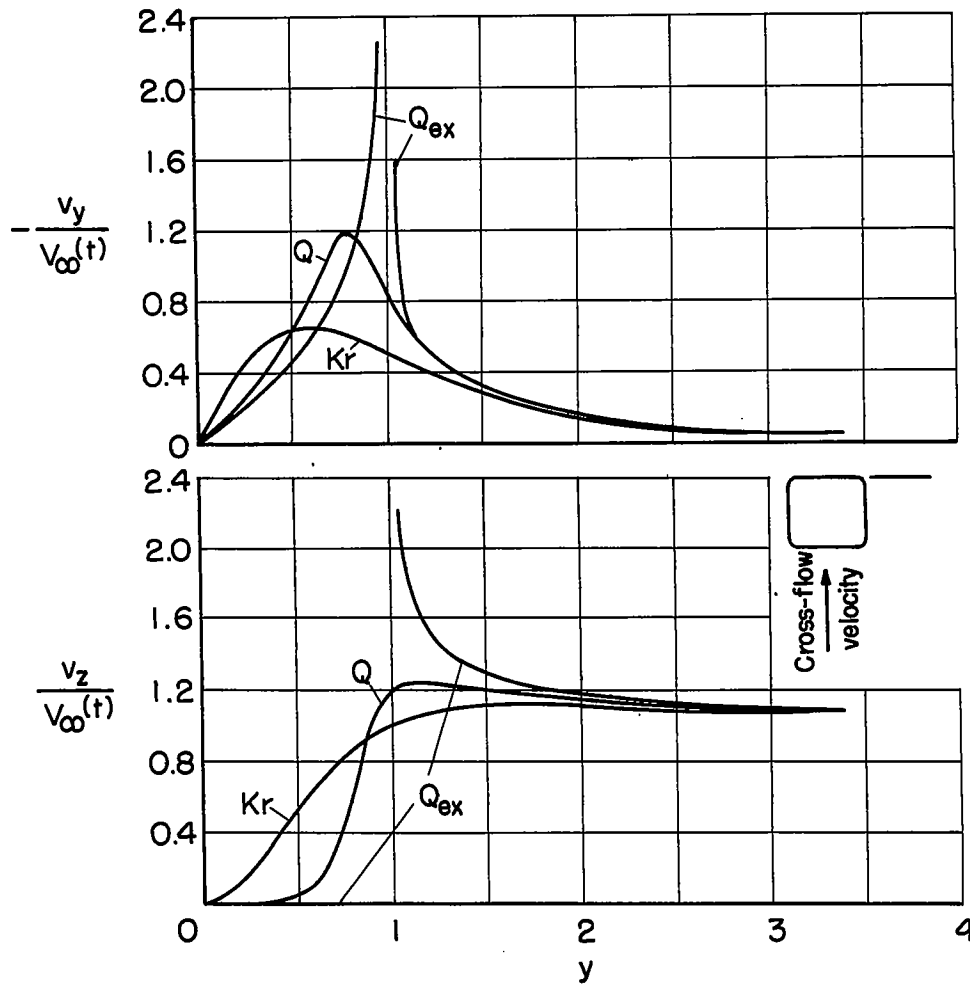
Figure 10.- Velocity field, comparison between circle, Q and Q_{ex}.
$2z_0/h_R = 1$ $\alpha_\infty^{(t)} = 90^\circ$.
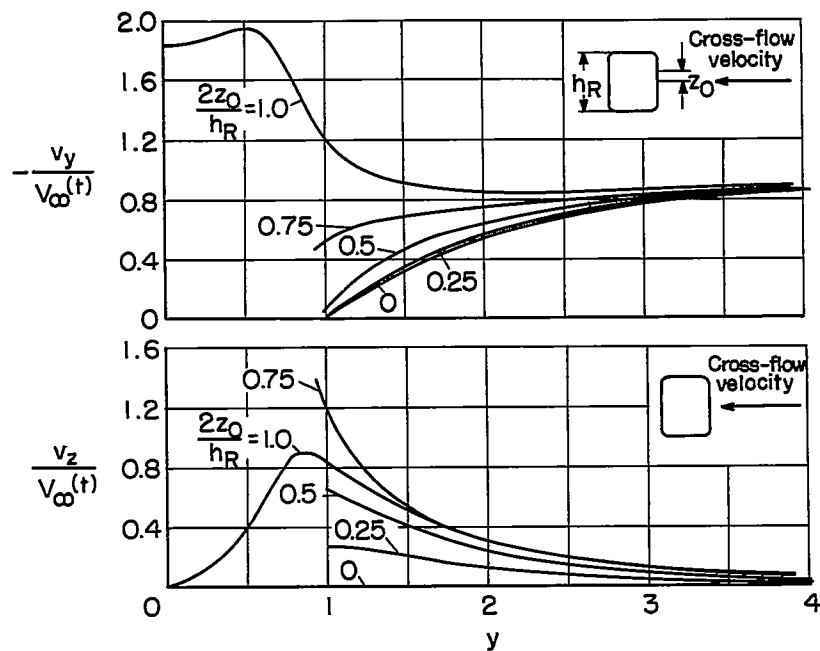
Figure 11.- Velocity field for rectangle R_1 in flow; $\alpha_\infty^{(t)} = 0^\circ$.
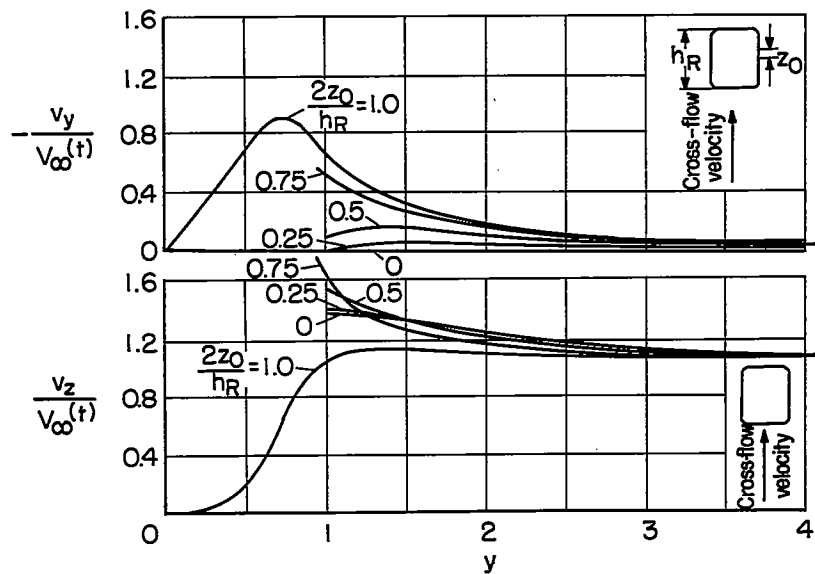
Figure 12.- Velocity field for rectangle R_1 in flow; $\alpha_\infty^{(t)} = 90^\circ$.
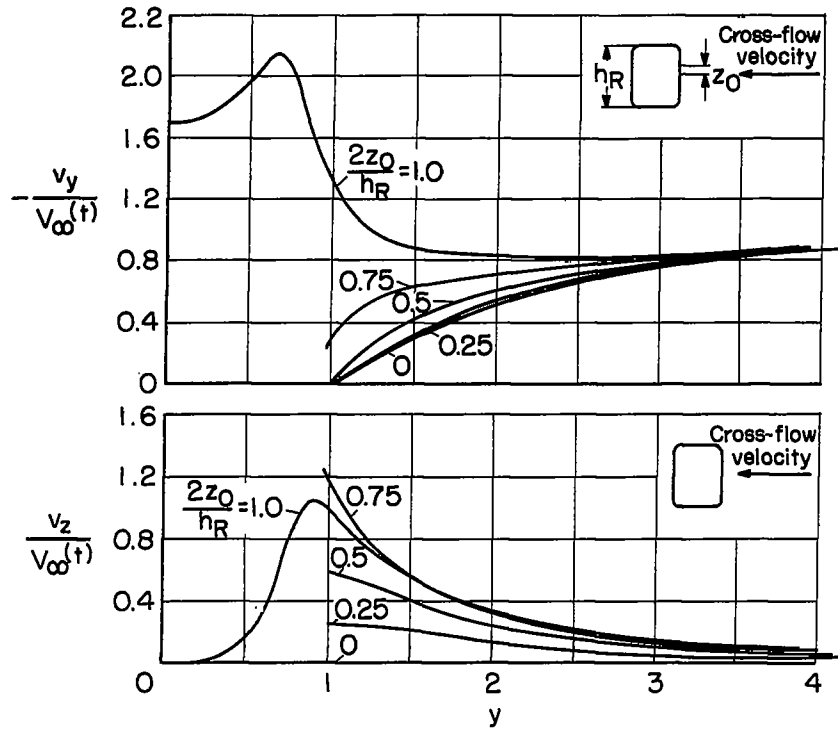
Figure 13.- Velocity field for rectangle R_2 in flow; $\alpha_\infty^{(t)} = 0°$.
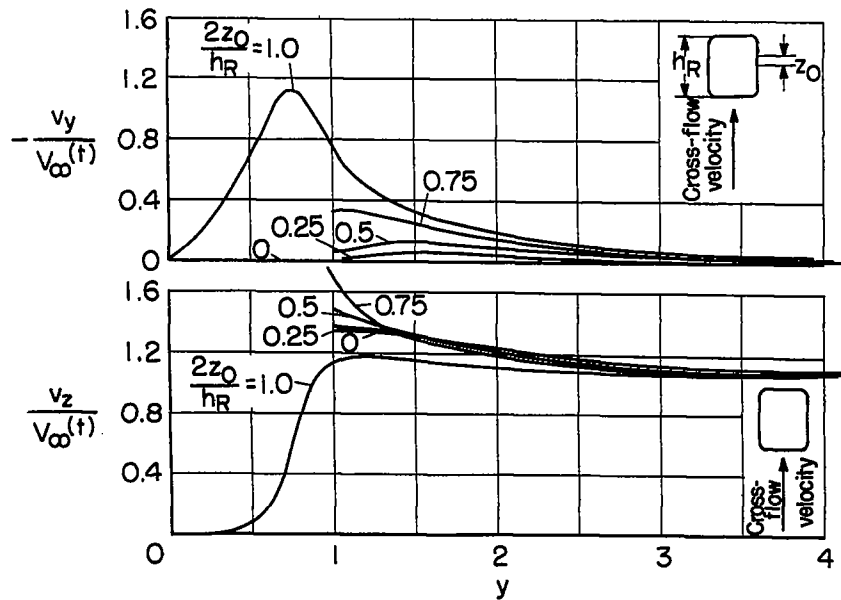
Figure 14.- Velocity field for rectangle R_2 in flow; $\alpha_\infty^{(t)} = 90°$.
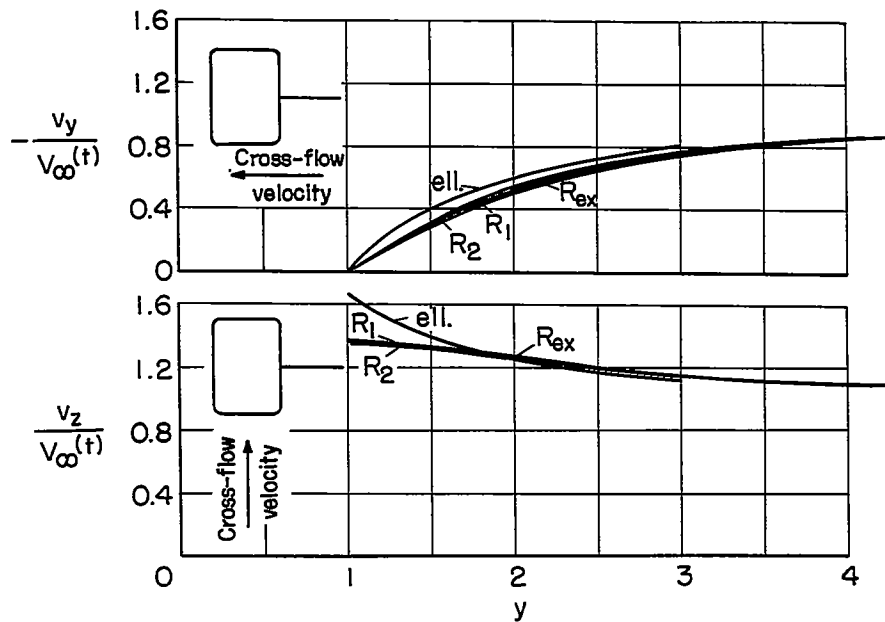
Figure 15.- Velocity field; comparison between ellipse, R_1, R_2, and R_{ex}. $2z_0/h_R = 0$ $\alpha_\infty^{(t)} = 0^\circ$, 90°.
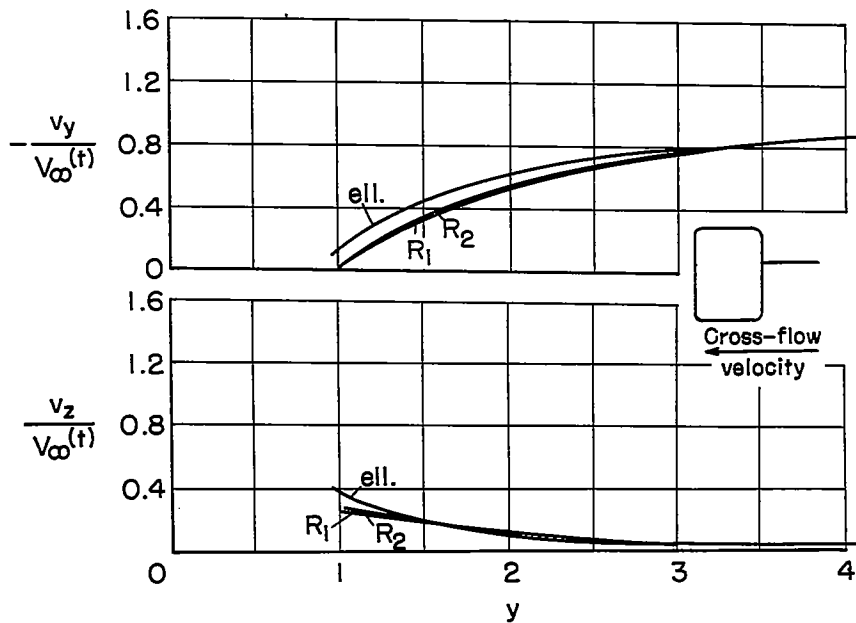
Figure 16.- Velocity field; comparison between ellipse, R_1, and R_2. $2z_0/h_R = 0.25$ $\alpha_\infty^{(t)} = 0^\circ$.
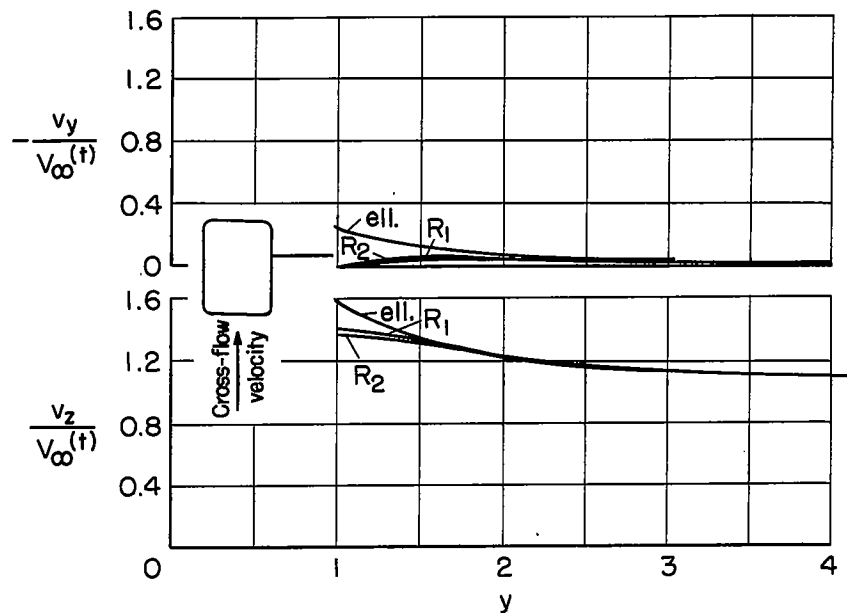
Figure 17.- Velocity field; comparison between ellipse, R_1, and R_2.
$2z_0/h_R = 0.25$ $\alpha_\infty^{(t)} = 90^\circ$.
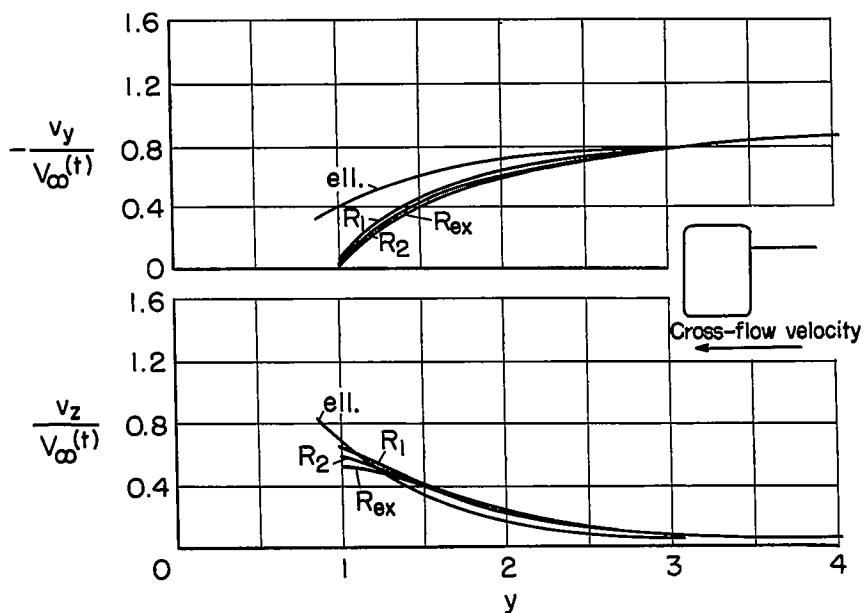

Figure 18.- Velocity field; comparison between ellipse, R_1, R_2, and
R_{ex}. $2z_0/h_R = 0.5$ $\alpha_\infty^{(t)} = 0^\circ$.
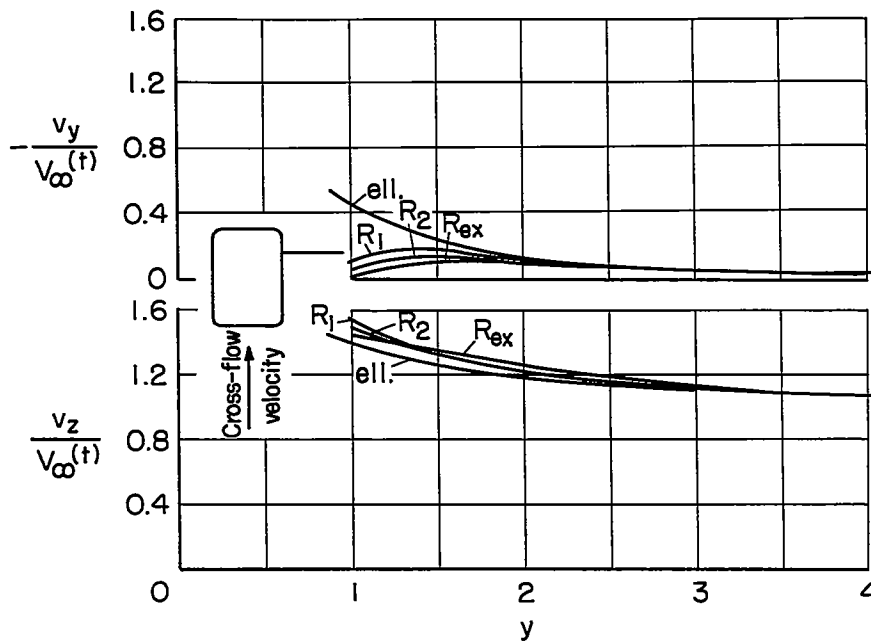
Figure 19.- Velocity field; comparison between ellipse, R_1, R_2, and R_{ex}. $2z_0/h_R = 0.5$ $\alpha_\infty^{(t)} = 90°$.
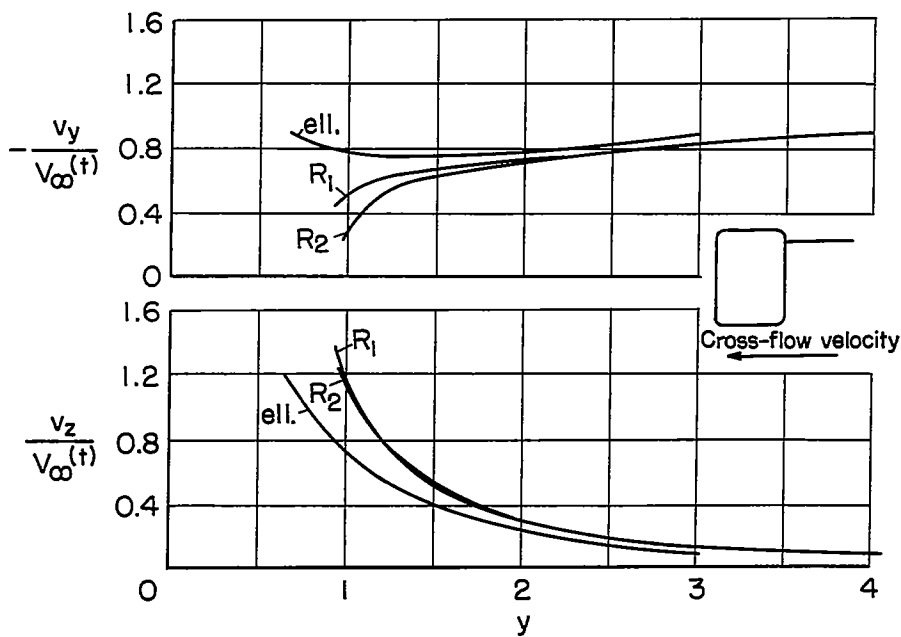
Figure 20.- Velocity field; comparison between ellipse, R_1 and R_2. $2z_0/h_R = 0.75$ $\alpha_\infty^{(t)} = 0°$.
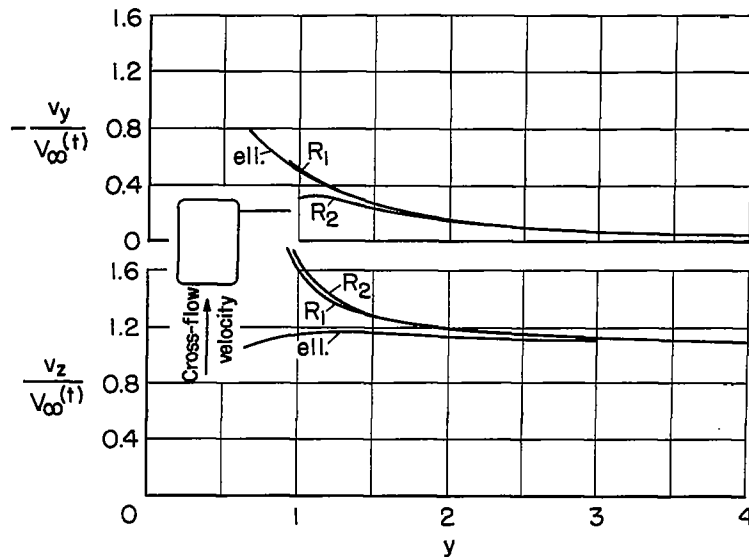
Figure 21.- Velocity field; comparison between ellipse, R_1 and R_2.
$2z_0/h_R = 0.75$ $\alpha_\infty^{(t)} = 90^\circ$.
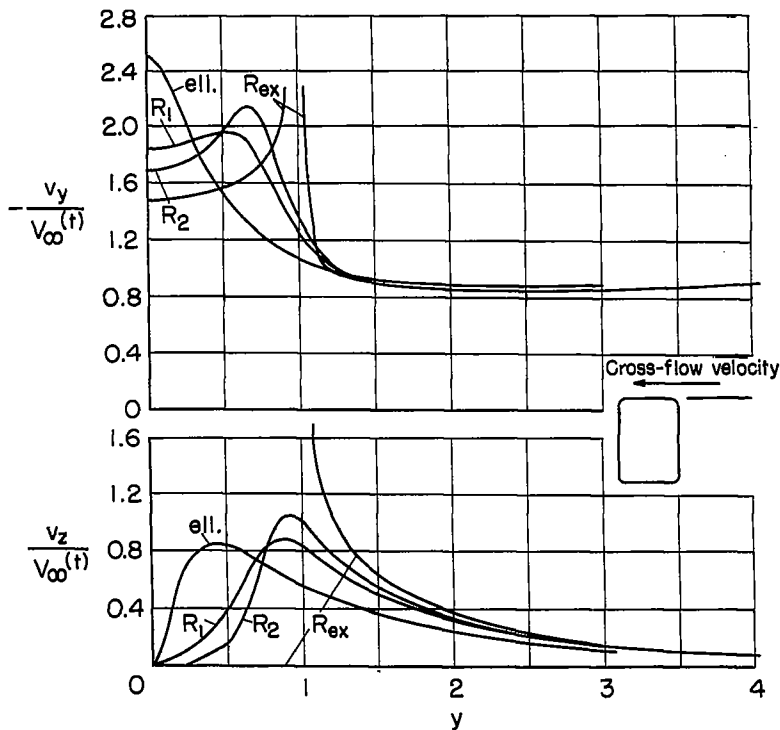
Figure 22.- Velocity field; comparison between ellipse, R_1, R_2, and
R_{ex}. $2z_0/h_R = 1$ $\alpha_\infty^{(t)} = 0^\circ$.
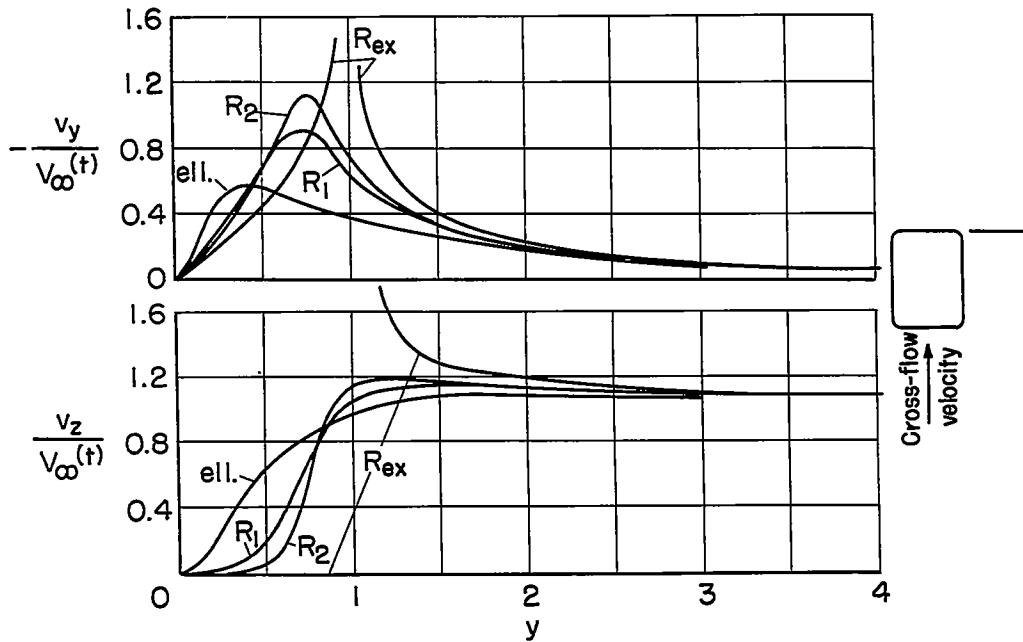
Figure 23.- Velocity field; comparison between ellipse, R_1, R_2, and R_{ex}. $2z_0/h_R = 1$ $\alpha_\infty^{(t)} = 90^0$.
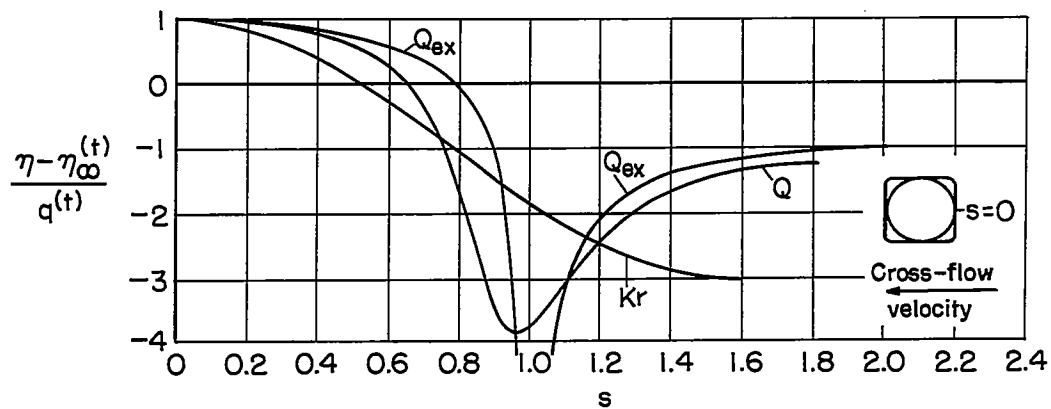
Figure 24.- Pressure distribution in the first quadrant on the contour of the circle. Q and Q_{ex}, drawn on the arc length. $\alpha_\infty^{(t)} = 0^0$.
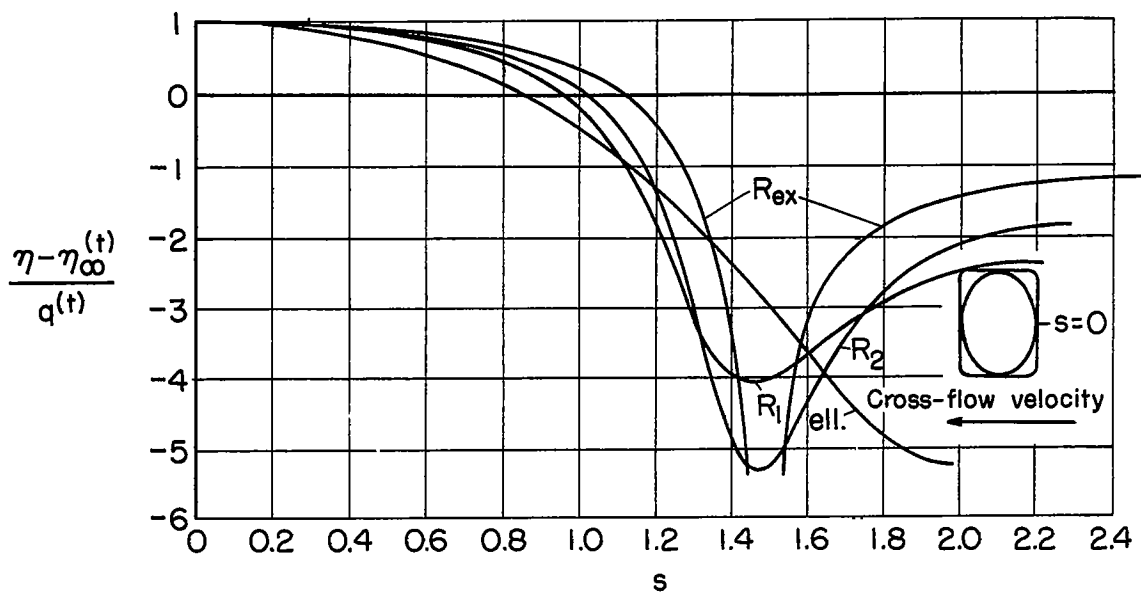
Figure 25.- Pressure distribution in the first quadrant on the contour of the ellipse, R_1, R_2, and R_{ex} drawn on the arc length. $\alpha_{\infty}^{(t)} = 0^{\circ}$.
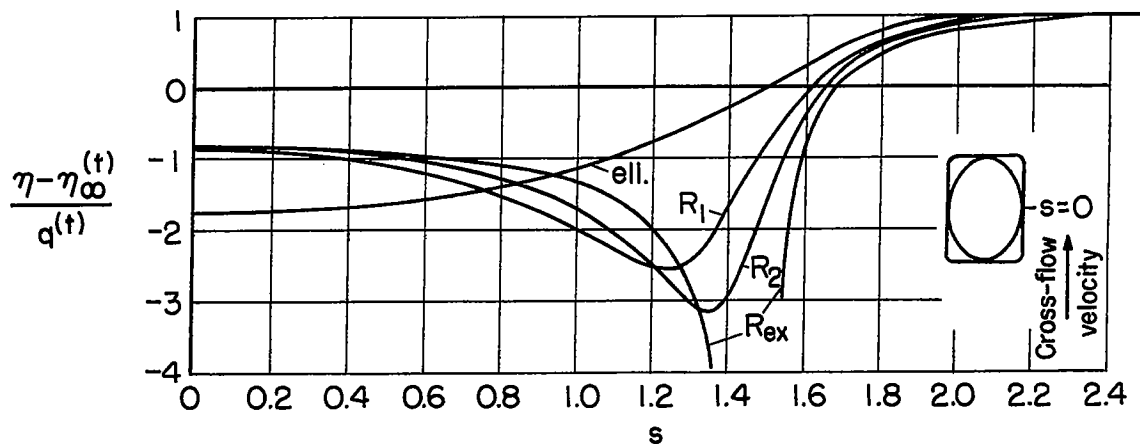
Figure 26.- Pressure distribution in the first quadrant on the contour of the ellipse, R_1, R_2, and R_{ex} drawn on the arc length. $\alpha_{\infty}^{(t)} = 90^{\circ}$.
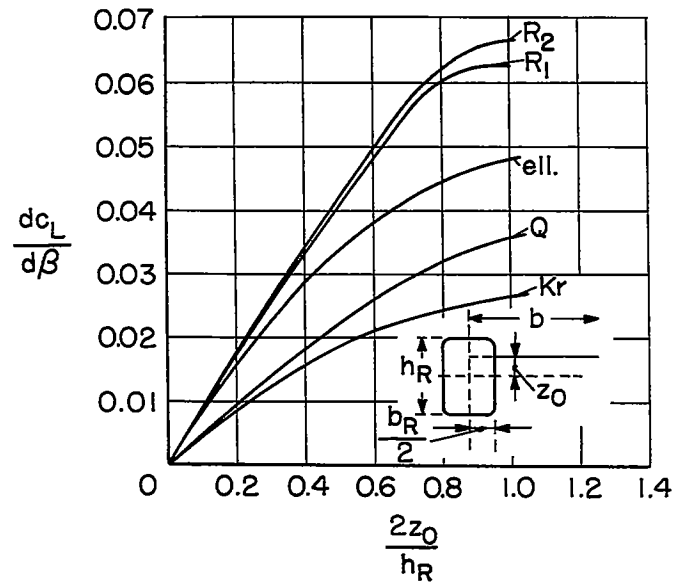
Figure 27.- Numerical coefficient of the rolling moment due to sideslip induced by the fuselage on an elliptical wing, depending on the vertical position of the wing.

$$c'_{a_\infty} = 5.5 \qquad \Lambda = 12.7 \qquad \lambda = 10 \qquad \frac{b_R}{b} = 1:15$$
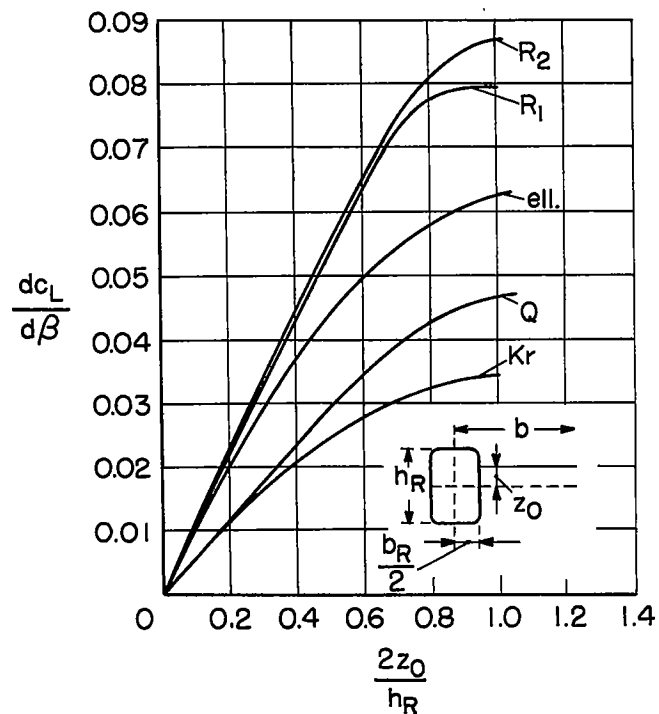
Figure 28.- Numerical coefficient of the rolling moment due to sideslip induced by the fuselage on an elliptical wing, depending on the vertical position of the wing.

$$c'_{a_\infty} = 5.5 \qquad \Lambda = 7.6 \qquad \lambda = 6 \qquad \frac{b_R}{b} = 1:12$$
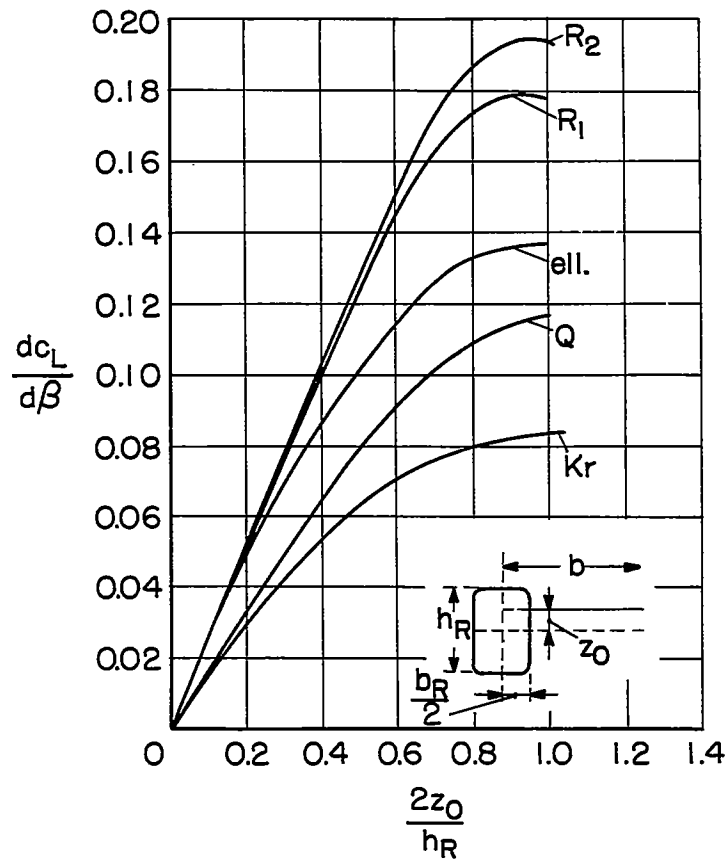
Figure 29.- Numerical coefficient of the rolling moment due to sideslip induced by the fuselage on an elliptical wing, depending on the vertical position of the wing.

$$c'_{a_\infty} = 5.5 \qquad \Lambda = 3.8 \qquad \lambda = 3 \qquad \frac{b_R}{b} = 1:6$$